

# TriSpec: Ternary Speculative Decoding via Lightweight Proxy Verification

Haoyun Jiang<sup>1,2</sup> Junqi He<sup>1</sup> Feng Hong<sup>1</sup> Xinlong Yang<sup>2</sup> Jianwei Zhang<sup>2</sup> Zheng Li<sup>2</sup> Zhengyang Zhuge<sup>2</sup>  
Zhiyong Chen<sup>1</sup> Bo Han<sup>3</sup> Junyang Lin<sup>2</sup> Jiangchao Yao<sup>1</sup>

## Abstract

Inference efficiency in Large Language Models (LLMs) is fundamentally limited by their serial, autoregressive generation, especially as reasoning becomes a key capability and response sequences grow longer. Speculative decoding (SD) offers a powerful solution, providing significant speed-ups through its lightweight drafting and parallel verification mechanism. While existing work has nearly saturated improvements in draft effectiveness and efficiency, this paper advances SD from a new yet critical perspective: the verification cost. We propose TriSpec, a novel ternary SD framework that, at its core, introduces a lightweight proxy to significantly reduce computational cost by approving easily verifiable draft sequences and engaging the full target model only when encountering uncertain tokens. TriSpec can be integrated with state-of-the-art SD methods like EAGLE-3 to further reduce verification costs, achieving greater acceleration. Extensive experiments on the Qwen3 and DeepSeek-R1-Distill-Qwen/LLaMA families show that TriSpec achieves up to 35% speedup over standard SD, with up to 50% fewer target model invocations while maintaining comparable accuracy.

## 1. Introduction

Large language models (LLMs) (Yang et al., 2025; Liu et al., 2024; Grattafiori et al., 2024) have made remarkable success on complex tasks, with recent advances in reasoning leading to longer and more sophisticated responses. This progress, however, is often hampered by the inherent latency of their serial, autoregressive generation process. Speculative decoding (SD) (Leviathan et al., 2023) addresses this efficiency bottleneck with a draft-then-verify paradigm. A small, fast drafter proposes candidate tokens, which the large target

<sup>1</sup>CMIC, Shanghai Jiao Tong University <sup>2</sup>Qwen Team, Alibaba Group <sup>3</sup>Hong Kong Baptist University. Correspondence to: Jiangchao Yao <sunarker@sjtu.edu.cn>.

Preprint. February 2, 2026.

model then verifies in a single parallel pass, significantly accelerating inference without compromising output quality.

Generally, the overall speedup in speculative decoding is governed by three key factors: the speed of draft token generation, the acceptance rate of draft tokens, and the speed of verification. Existing work has made substantial progress on the first two factors. Medusa (Cai et al., 2024) and EAGLE (Li et al., 2024a) propose lightweight drafter architectures, shortening the compute path and making the drafting time almost negligible. Building on this design, subsequent methods further improve acceptance rates by optimizing candidate paths (Li et al., 2024b; Zhang et al., 2024b), refining training paradigms (Zhang et al., 2024a; Li et al., 2025; Liu et al., 2024), or relaxing verification constraints (Bachmann et al., 2025; Narasimhan et al., 2024), pushing this factor close to saturation. In contrast, the *verification speed* remains an equally crucial yet largely overlooked factor. This gap motivates us to explore *whether the verification role of the large target model could be effectively handled by a much more efficient, lightweight verifier*.

Our answer to this question is affirmation. We find that smaller models from the same family as the target model (e.g., Qwen3-1.7B and Qwen3-32B) show significant potential, as they exhibit a high degree of alignment with the output distribution (§3.1). Consequently, a small model can reliably replaces the target model for verifying the majority of tokens, and the challenge lies in a small subset of tokens where their capabilities diverge. Fortunately, we find that a proper measure like a specific margin metric can sufficiently characterize the capability boundary, and route the verification task between a large target model and its smaller surrogate (Figure 2(b)).

Based on these insights, we propose TriSpec, a ternary speculative decoding paradigm that coordinates three models with complementary roles. A single-layer drafter provides high-throughput drafting; a lightweight proxy verifier quickly pre-verifies the draft and locally corrects a subset of tokens; and a large verifier supplies authoritative verification when needed (Figure 1). By delegating a substantial portion of verification to the cheaper proxy, TriSpec effectively reduces per-round verification time and thus the overall decoding latency. Extensive experiments on Qwen3 and

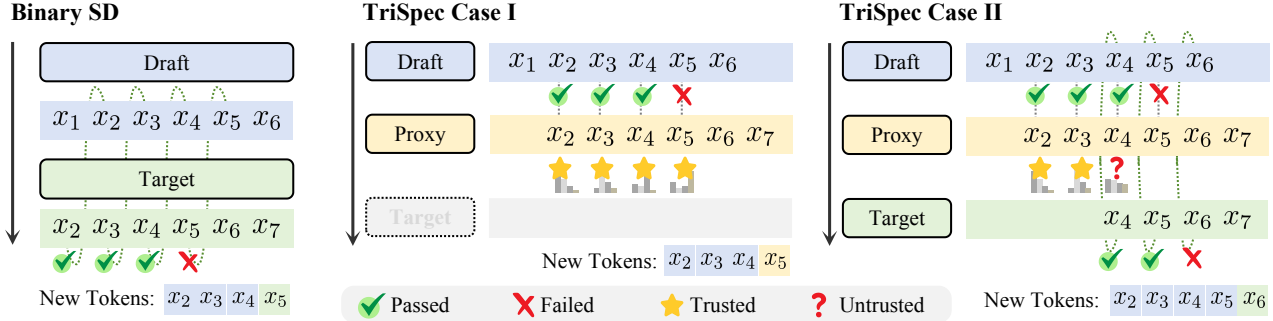


Figure 1. Comparison of standard speculative decoding and TriSpec. Case I: The proxy verifier provides local correction of drafts, bypassing the large-scale target model to gain speed. Case II: If the proxy’s verification is deemed untrusted before the first rejection, the corresponding tokens are escalated to the target model for authoritative validation to ensure accuracy. TriSpec employs a margin-based criterion to classify proxy verification as trusted or untrusted.

DeepSeek-R1-Distill-Qwen/LLaMA families demonstrate that TriSpec delivers significant speedups over SOTA speculative decoding methods. In summary, our contributions are summarized as follows:

- We identify the verification cost as a new and critical perspective for accelerating speculative decoding, and show that smaller models within the same family exhibit strong alignment with their larger counterparts, making them effective and lightweight proxy verifiers.
- We introduce TriSpec, a ternary speculative decoding paradigm that jointly orchestrates a drafter, a proxy verifier, and the target model. A margin-based routing rule adaptively allocates verification and invokes the expensive target only when necessary, preserving accuracy while substantially reducing verification overhead.
- Extensive experiments on popular models and benchmarks show that TriSpec achieves up to a 35% speedup over standard speculative decoding while reducing target-model invocations by more than half, with an average accuracy degradation of less than 1%.

## 2. Rethinking Speculative Decoding Speedup

### 2.1. Speculative Decoding

Standard speculative decoding follows a draft-then-verify paradigm with two models: a draft model  $\mathcal{M}_d$  and a target model  $\mathcal{M}_t$ . Let  $\mathcal{V}$  denote a finite vocabulary with size  $V := |\mathcal{V}|$ , and let the current decoding prefix be  $X \in \mathcal{V}^l$ , including both the prompt and previously generated tokens.

**Drafting phase.** During drafting,  $\mathcal{M}_d$  autoregressively produces  $k$  draft tokens and their probability distributions:

$$(x_1^{(d)}, \mathbf{p}_1^{(d)}), \dots, (x_k^{(d)}, \mathbf{p}_k^{(d)}) \leftarrow \mathcal{M}_d(X), \quad (1)$$

where each  $\mathbf{p}_i^{(d)} \in \mathbb{R}^V$  is the softmax probability distribution produced by the draft model at position  $i$  and  $x_i^{(d)} \in \mathcal{V}$

is sampled from  $\mathbf{p}_i^{(d)}$ . For a distribution  $\mathbf{p}$  and token  $x \in \mathcal{V}$ , we write  $\mathbf{p}(x)$  for the probability assigned to  $x$ .

**Verification phase.** In the verification stage, the target model  $\mathcal{M}_t$  evaluates the  $k$  drafted tokens in a single parallel forward pass:

$$(x_1^{(t)}, \mathbf{p}_1^{(t)}), (x_2^{(t)}, \mathbf{p}_2^{(t)}), \dots, (x_{k+1}^{(t)}, \mathbf{p}_{k+1}^{(t)}) \leftarrow \mathcal{M}_t(x_1^{(d)}, x_2^{(d)}, \dots, x_k^{(d)} \mid X) \quad (2)$$

where  $x_i^{(t)} \in \mathcal{V}$  and  $\mathbf{p}_i^{(t)} \in \mathbb{R}^V$  denote the target token and its probability distribution at position  $i$ , respectively. Each drafted token  $x_i^{(d)}$  is accepted with probability  $\min(1, \mathbf{p}_i^{(t)}(x_i)/\mathbf{p}_i^{(d)}(x_i))$ . If any rejection occurs, all drafted tokens to its right are discarded, and a replacement token is sampled from the normalized positive residual norm( $\max(0, \mathbf{p}_i^{(t)} - \mathbf{p}_i^{(d)})$ ) at the first rejection position. Prior work (Chen et al., 2023) proves that speculative sampling exactly matches the output distribution of naive target-model decoding, and is thus provably lossless.

### 2.2. Latency Analysis of Speculative Decoding

**Lemma 2.1** (Latency decomposition for SD). *Consider a speculative decoding process that generates  $N$  tokens. Let  $\tau$  denote the average acceptance length (tokens accepted per verification round), and let  $t_d$ ,  $t_v$ , and  $t_o$  be the average per-round drafting time, verification time, and other overhead, respectively. Then the end-to-end latency satisfies*

$$L = \frac{N}{\tau} (t_d + t_v + t_o). \quad (3)$$

*In practice,  $t_o$  is typically small and nearly constant compared to  $t_d$  and  $t_v$ , and  $N$  can be regarded as approximately constant for a given model. Consequently,*

$$L \propto \frac{t_d + t_v}{\tau}. \quad (4)$$

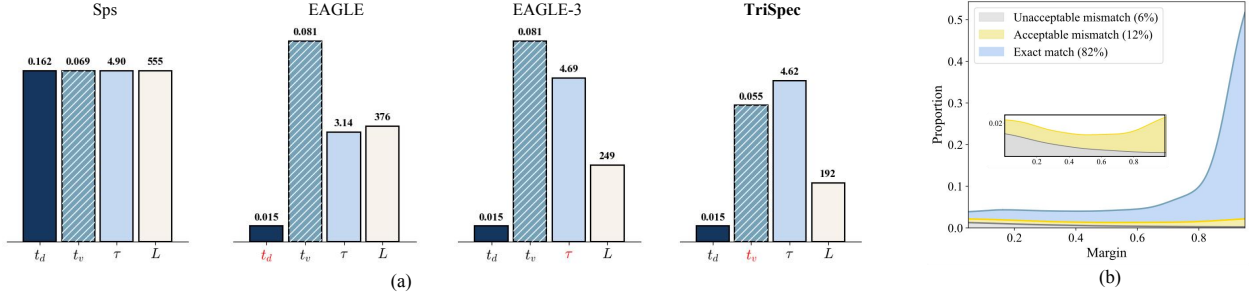


Figure 2. (a) Latency decomposition of speculative decoding across representative methods. EAGLE reduces drafting cost  $t_d$  via a single-layer design. EAGLE-3 and related methods further enlarge the acceptance length  $\tau$  by improving draft token quality. Our proposed TriSpec introduces a new perspective by reducing the verification cost  $t_v$ . (b) Distribution of token outcomes versus the proxy’s top-1-top-2 probability margin on ShareGPT. Areas are stacked and globally normalized, so the total across all classes sums to 1.

**Remark.** As modern speculative decoding methods substantially reduce  $t_d$  and increase  $\tau$ , reducing the per-round verification time  $t_v$  becomes an important and promising direction for further acceleration.

**Drafting has been largely optimized.** Recent latency reductions have primarily been achieved by decreasing  $t_d$  and increasing  $\tau$ . Early SD used a separate small model as the drafter, but its multi-layer architecture made drafting latency-dominant (Figure 2(a), Sps). Single-layer drafter designs, such as Medusa and EAGLE, greatly reduce  $t_d$  while maintaining a high  $\tau$  (Figure 2(a), EAGLE), making them the prevailing approach. Subsequent work further increase  $\tau$  by using tree-structure candidate paths and enhanced training schemes, such as EAGLE-3 (Figure 2(a), EAGLE-3). With Multi-Token Prediction (MTP) (Liu et al., 2024) integrating draft-model training into pre-training, the acceptance rate of draft tokens can even reach up to 90%.

**Verification remains the dominant bottleneck.** Little progress has been made in directly reducing the per-round verification time  $t_v$ . In state-of-the-art pipelines (e.g., EAGLE-3), verification time has become the dominant source of per-round latency, as each target-model invocation traverses a long computational path with a large parameter budget. A straightforward idea is to employ a lightweight verifier to offload part of the verification from the target, thereby reducing the average verification time across rounds.

### 3. TriSpec

In this section, we propose TriSpec, a tightly-coupled ternary speculative decoding framework guided by a simple principle: *use the cheapest component to fulfill each role*. Specifically, TriSpec integrates a *single-layer drafter* for low-cost token generation, a *lightweight proxy verifier* to rapidly validate easy tokens and flag uncertain ones, and the *target model* for exact verification of flagged cases to ensure correctness. By properly offloading most verification

from the target to the proxy, TriSpec reduces the effective per-round verification time  $t_v$  while maintaining accuracy.

#### 3.1. Proxy choice: same-family smaller models

We identify smaller same-family models as ideal proxy verifiers, justified by the following three core properties.

**Strong Alignment.** Because SD verifies tokens individually, we assess token-level alignment between the proxy and the target model on the ShareGPT dataset using Qwen3-family models. At each position, we compare the proxy’s prediction of the next token with the target’s and classify the results into three categories: exact match (same token), acceptable mismatch (different token but considered acceptable by a stronger LLM), and unacceptable mismatch (otherwise). The experiment details are provided in Appendix C.2. Under this protocol, the proxy achieves 82% exact match with the target (EAGLE-3 drafter: 68%), with only 6% of tokens deemed unacceptable, demonstrating a strong alignment at the token level.

**Trustworthy outputs.** Beyond strong alignment with the target, the proxy’s outputs are themselves trustworthy. In the standalone example (Appendix C.1), despite phrasing differences, the proxy and target reach the same final answer, indicating that modest token-level discrepancies between them are tolerable. Consistently, the end-to-end relaxed-verification experiments (Appendix C.3) show that limited deviations from the target do not materially affect accuracy.

**Clear Separability.** A crucial property for an intermediate verifier is the existence of a clear indicator to distinguish between trusted and uncertain outputs. We find that the margin between the proxy’s top-1 and top-2 probabilities serves this purpose effectively. As shown in Figure 2(b), this confidence margin cleanly stratifies tokens: a large margin (e.g.,  $> 0.5$ ) correlates strongly with acceptable predictions, while unacceptable tokens are concentrated in low-margin cases. This property provides a robust and actionable criterion for assessing the reliability of the proxy’s verification.

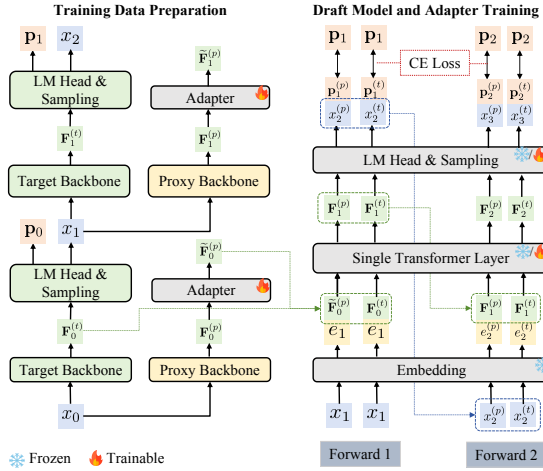


Figure 3. Training pipeline of the draft model and adapter in TriSpec. The green, yellow, and gray modules represent the target, proxy, and drafter components, respectively.

### 3.2. Ternary speculative decoding

**Drafter selection and adapter training.** We adopt the EAGLE single-layer architecture as our draft model for its state-of-the-art efficiency. To support TriSpec’s proxy-based verification, the drafter must flexibly process features from either the target or the proxy model. As in Figure 3, we augment the EAGLE architecture with a one-layer MLP adapter that maps proxy features into the drafter’s expected feature space. This architecture supports two training regimes: (i) *joint training*, where the drafter and adapter are optimized together using both proxy and target features; and (ii) *adapter-only finetuning*, where a pretrained drafter’s weights are fixed and only the adapter is trained using proxy features. We compare these regimes in Section 4.4.

**Proxy pre-verification.** Given the drafted pairs  $(x_1^{(d)}, \mathbf{p}_1^{(d)}), \dots, (x_k^{(d)}, \mathbf{p}_k^{(d)})$ , we leverage the proxy  $\mathcal{M}_p$  to perform a single parallel pass and returns its own token predictions and distributions:

$$(x_1^{(p)}, \mathbf{p}_1^{(p)}), (x_2^{(p)}, \mathbf{p}_2^{(p)}), \dots, (x_{k+1}^{(p)}, \mathbf{p}_{k+1}^{(p)}) \quad (5)$$

$$\leftarrow \mathcal{M}_p(x_1^{(d)}, x_2^{(d)}, \dots, x_k^{(d)} \mid X),$$

where  $x_i^{(p)} \in \mathcal{V}$  and  $\mathbf{p}_i^{(p)} \in \mathbb{R}^V$  are the proxy's predicted token and its softmax distribution. Following standard speculative decoding, the proxy determines acceptance by comparing its probability distribution with that of the drafter. Formally, for each draft token  $x_i^{(d)}$  where  $i \in \{1, \dots, k\}$ , we define a Bernoulli acceptance variable

$$s_i \sim \text{Bernoulli} \left( \min \left\{ 1, \frac{\mathbf{p}_i^{(p)}(x_i^{(d)})}{\mathbf{p}_i^{(d)}(x_i^{(d)})} \right\} \right), \quad (6)$$

which in the greedy case reduces to  $s_i = \mathbf{1}\{x_i^{(p)} = x_i^{(d)}\}$ .

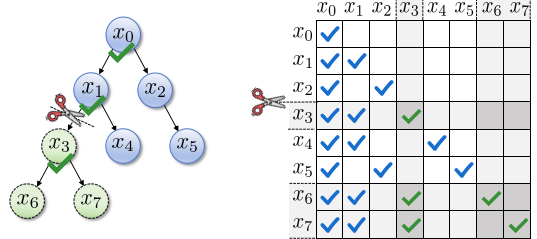


Figure 4. Token pruning and attention mask updates in TriSpec.

Then, the proxy-side acceptance length is

$$\tau_a = \min \left( \{ i \mid 0 \leq i \leq k-1, s_{i+1} = 0 \} \cup \{k\} \right). \quad (7)$$

**Margin-based Criterion.** To preserve predictive integrity, TriSpec must identify scenarios where the proxy’s verification is likely to diverge from the target model. As established in §3.1, the confidence margin between the proxy’s top-1 and top-2 probabilities serves as a robust signal for this alignment. We thus define a margin-based binary predicate  $g : \mathbb{R}^V \rightarrow \{0, 1\}$  to determine whether a proxy verification result can be trusted:

$$g(\mathbf{p}_i^{(p)}) = \mathbf{1} \left\{ \text{top}_1(\mathbf{p}_i^{(p)}) - \text{top}_2(\mathbf{p}_i^{(p)}) \geq \lambda \right\}, \quad (8)$$

where  $i \in \{1, \dots, k+1\}$ ,  $\text{top}_1(x)$  and  $\text{top}_2(x)$  denote the largest and second-largest entries of  $x$ , and  $\lambda \in (0, 1)$  is a tunable threshold controlling the accuracy-latency trade-off. To measure how long we can rely on the proxy before escalation, we define the proxy-trusted prefix length as the longest initial segment that passes the margin test:

$$\tau_m = \min(\{i \mid 0 \leq i \leq k, g(\mathbf{p}_{i+1}^{(p)}) = 0\} \cup \{k+1\}). \quad (9)$$

In particular, if  $g(\mathbf{p}_i^{(p)}) = 1$  for all  $i$ , then  $\tau_m = k + 1$ , indicating that the proxy's verification is trusted for the entire draft and can reliably produce the  $(k + 1)$ -th token.

**Adaptive Verification Routing.** Based on the proxy-side acceptance length  $\tau_a$  and the proxy-trusted prefix length  $\tau_m$ , TriSpec adaptively routes the verification into two cases:

(i) If  $\tau_a < \tau_m$ , the proxy's verification remains trustworthy at the first rejection point, and it can complete the verification round without invoking the target model (Figure 1 center). Accordingly, we accept  $x_{1:\tau_a}^{(d)}$  and locally correct the next token by replacing it with  $x_{\tau_a+1}^{(p)}$ . The generated sequence for this round is  $Y = \{x_1^{(d)}, \dots, x_{\tau_a}^{(d)}, x_{\tau_a+1}^{(p)}\}$ .

(ii) If  $\tau_a \geq \tau_m$ , the proxy's verification is deemed untrusted before the first rejection point, so the verification is thus delegated to the target model (Figure 1 right). We first accept  $x_{1:t_m}^{(d)}$ , prune these tokens from the draft tree (Figure 4, and pass the remaining branches to the target for validation:

$$(x_{\tau_m+1}^{(t)}, \mathbf{p}_{\tau_m+1}^{(t)}), \dots, (x_{k+1}^{(t)}, \mathbf{p}_{k+1}^{(t)}) \quad (10)$$

$$\leftarrow \mathcal{M}_t(x_{\tau_m+1}^{(d)}, \dots, x_k^{(d)} \mid X, x_{1:\tau_m}^{(d)}),$$

Table 1. Accuracy and speedup of different methods on five reasoning benchmarks, evaluated with a sampling temperature of 0. “SC” denotes the SpecCascade baseline. “HASS/EAGLE3 + TriSpec” refers to a draft model trained under the HASS or EAGLE3 pipeline and employing TriSpec for proxy-based verification.

Model	Method	GSM8K		MATH500		GK23-en		HumanEval		MBPP		Avg	
		Acc.	Speedup	Acc.	Speedup	Acc.	Speedup	Acc.	Speedup	Acc.	Speedup	Acc.	Speedup
Qwen3	Single Model (Target,32B)	98%	1.00×	85%	1.00×	75%	1.00×	87%	1.00×	77%	1.00×	84.4%	1.00×
	Single Model (Proxy,1.7B)	86%	2.36×	81%	3.01×	70%	3.03×	81%	2.93×	51%	2.92×	73.8% -10.6%	2.85×
	HASS	98%	2.98×	86%	2.27×	74%	2.30×	87%	2.03×	77%	2.18×	84.4% ±0%	2.35×
	HASS + SC[Chow]	80%	3.33×	55%	2.60×	51%	2.64×	74%	2.23×	56%	2.33×	63.2% -21.2%	2.63×
	HASS + SC[OPT]	76%	3.25×	38%	2.66×	33%	2.65×	49%	2.30×	20%	2.34×	43.2% -41.2%	2.64×
	HASS + SC[Token]	98%	3.10×	86%	2.34×	74%	2.39×	87%	2.15×	74%	2.28×	83.8% -0.6%	2.63×
	HASS + TriSpec	97%	<b>3.85</b> ×	86%	<b>3.18</b> ×	75%	<b>3.26</b> ×	86%	<b>2.99</b> ×	74%	<b>2.80</b> ×	83.6% -0.8%	<b>3.22</b> ×
	EAGLE3	98%	3.25×	87%	2.73×	74%	2.77×	87%	2.71×	76%	2.77×	84.4% ±0%	2.85×
	EAGLE3 + SC[Chow]	95%	3.39×	70%	2.91×	58%	2.94×	76%	2.82×	67%	2.85×	73.2% -11.2%	2.98×
	EAGLE3 + SC[OPT]	93%	3.43×	58%	3.06×	42%	3.01×	61%	2.91×	49%	2.87×	60.6% -23.8%	3.06×
DSQ	EAGLE3 + SC[Token]	98%	3.34×	86%	2.90×	74%	2.91×	87%	2.78×	76%	2.85×	84.2% -0.2%	2.96×
	EAGLE3 + TriSpec	98%	<b>4.18</b> ×	88%	<b>3.49</b> ×	74%	<b>3.55</b> ×	87%	<b>3.27</b> ×	74%	<b>3.24</b> ×	84.2% -0.2%	<b>3.55</b> ×
	Single Model (Target,32B)	93%	1.00×	86%	1.00×	74%	1.00×	85%	1.00×	72%	1.00×	82.0%	1.00×
	Single Model (Proxy,1.5B)	72%	3.09×	76%	3.32×	62%	3.33×	54%	3.22×	38%	3.32×	60.4% -21.6%	3.26×
	HASS	93%	3.28×	88%	2.99×	72%	2.90×	84%	2.78×	73%	3.02×	82.0% ±0%	2.99×
	HASS + SC[Chow]	77%	3.46×	51%	3.22×	44%	3.06×	75%	2.85×	62%	3.10×	61.8% -20.2%	3.14×
	HASS + SC[OPT]	77%	3.59×	39%	3.20×	20%	3.18×	41%	2.88×	18%	3.12×	39.0% -43.0%	3.19×
	HASS + SC[Token]	91%	3.41×	85%	3.13×	69%	2.96×	84%	2.80×	72%	3.04×	80.2% -1.8%	3.07×
	HASS + TriSpec	91%	<b>3.76</b> ×	87%	<b>3.41</b> ×	74%	<b>3.33</b> ×	85%	<b>2.98</b> ×	71%	<b>3.24</b> ×	81.6% -0.4%	<b>3.34</b> ×
	EAGLE3	93%	3.42×	88%	3.19×	74%	3.11×	86%	3.09×	72%	3.27×	82.6% +0.6%	3.22×
DSL	EAGLE3 + SC[Chow]	84%	3.67×	69%	3.47×	51%	3.43×	72%	3.19×	64%	3.33×	68.0% -14.0%	3.42×
	EAGLE3 + SC[OPT]	81%	3.69×	58%	3.51×	45%	3.46×	54%	3.23×	48%	3.33×	57.2% -24.8%	3.44×
	EAGLE3 + SC[Token]	92%	3.54×	82%	3.36×	72%	3.26×	86%	3.18×	70%	3.27×	80.4% -1.6%	3.32×
	EAGLE3 + TriSpec	91%	<b>4.14</b> ×	88%	<b>3.69</b> ×	75%	<b>3.63</b> ×	88%	<b>3.32</b> ×	69%	<b>3.57</b> ×	82.2% +0.2%	<b>3.67</b> ×
	Single Model (Target,70B)	88%	1.00×	90%	1.00×	78%	1.00×	87%	1.00×	79%	1.00×	84.4%	1.00×
	Single Model (Proxy,8B)	77%	3.71×	83%	3.73×	73%	4.01×	80%	3.89×	59%	4.03×	74.4% -20.0%	3.87×
	EAGLE3	88%	2.83×	89%	2.35×	76%	2.31×	84%	2.49×	80%	2.40×	83.4% -1.0%	2.48×
	EAGLE3 + SC[Chow]	82%	2.90×	81%	2.50×	65%	2.61×	74%	2.58×	71%	2.57×	74.6% -9.8%	2.63×
	EAGLE3 + SC[OPT]	78%	3.02×	66%	2.84×	48%	2.93×	60%	2.89×	51%	2.91×	60.6% -23.8%	2.92×
	EAGLE3 + SC[Token]	87%	2.92×	88%	2.43×	75%	2.56×	85%	2.69×	78%	2.65×	82.6% -1.8%	2.65×
	EAGLE3 + TriSpec	86%	<b>3.74</b> ×	88%	<b>3.35</b> ×	77%	<b>3.36</b> ×	87%	<b>3.07</b> ×	76%	<b>3.29</b> ×	82.8% -1.6%	<b>3.36</b> ×

Applying the standard left-to-right acceptance rule to  $\mathbf{p}^{(t)}$  yields the target-verified acceptance length  $\tau_t$ . The generated sequence for this round is  $Y = \{x_1^{(d)}, \dots, x_{\tau_m + \tau_t}^{(d)}, x_{\tau_m + \tau_t + 1}^{(t)}\}$ .

### 3.3. Further Discussion of TriSpec

TriSpec aligns with the paradigm of verification-side optimization, sharing the core philosophy of trading marginal accuracy for increased throughput by relaxing verification constraints. However, it diverges fundamentally from mainstream approaches like Judge Decoding and SpecCascade in its optimization objective. While prior methods aim to extend the average acceptance length  $\tau$  by tolerating misaligned but high-quality tokens, TriSpec minimizes  $t_v$  by offloading simple tokens to the proxy, thereby reducing expensive target model invocations.

This focus on  $t_v$  optimization is particularly effective when

paired with high-efficiency drafters (e.g., EAGLE-3 and MTP). Because these drafters are intrinsically tied to target-model features, their predictive quality typically diminishes as the draft length increases, which inherently constrains the potential for further  $\tau$  extension via traditional relaxation. Notably, this constraint is explicitly acknowledged in the limitations section of the Judge Decoding paper (Bachmann et al., 2025). In contrast, TriSpec’s mechanism remains largely agnostic to the specific quality of the draft distribution, ensuring versatility across diverse drafting architectures. Furthermore, TriSpec is characterized by mutual alignment among all three components, enabling direct pairwise interactions that contrast with the strictly linear flow of cascaded speculative decoding frameworks such as Tri-Force (Sun et al., 2024). This ternary synergy facilitates more sophisticated cross-model coordination, significantly reducing the frequency of expensive target model invocations while preserving robust reasoning performance.

Table 2. Accuracy and speedup of different methods on five reasoning benchmarks, evaluated with a sampling temperature of 1.

Model	Method	GSM8K		MATH500		GK23-en		HumanEval		MBPP		Avg	
		Acc.	Speedup	Acc.	Speedup	Acc.	Speedup	Acc.	Speedup	Acc.	Speedup	Acc.	Speedup
Qwen3	Single Model (Target,32B)	98%	1.00 $\times$	85%	1.00 $\times$	76%	1.00 $\times$	87%	1.00 $\times$	76%	1.00 $\times$	84.4%	1.00 $\times$
	Single Model (Proxy,1.7B)	88%	2.62 $\times$	80%	2.84 $\times$	73%	2.90 $\times$	76%	2.90 $\times$	61%	2.90 $\times$	75.6%	-8.8%
	HASS	96%	2.61 $\times$	86%	2.05 $\times$	75%	2.05 $\times$	88%	1.96 $\times$	74%	1.94 $\times$	83.8%	-0.6%
	HASS + TriSpec	95%	<b>3.01</b> $\times$	84%	<b>2.51</b> $\times$	77%	<b>2.54</b> $\times$	89%	<b>2.31</b> $\times$	72%	<b>2.25</b> $\times$	83.4%	-1.0%
DSQ	EAGLE3	98%	2.78 $\times$	84%	2.55 $\times$	77%	2.52 $\times$	86%	2.58 $\times$	74%	2.52 $\times$	83.8%	-0.6%
	EAGLE3 + TriSpec	96%	<b>3.33</b> $\times$	86%	<b>3.06</b> $\times$	76%	<b>3.13</b> $\times$	88%	<b>2.94</b> $\times$	73%	<b>2.93</b> $\times$	83.8%	-0.6%
	Single Model (Target,32B)	92%	1.00 $\times$	88%	1.00 $\times$	77%	1.00 $\times$	88%	1.00 $\times$	76%	1.00 $\times$	84.2%	1.00 $\times$
	Single Model (Proxy,1.5B)	71%	2.99 $\times$	78%	2.91 $\times$	66%	3.15 $\times$	62%	3.12 $\times$	47%	3.11 $\times$	64.8%	-19.4%
DSL	HASS	90%	2.97 $\times$	87%	2.19 $\times$	76%	2.33 $\times$	90%	1.98 $\times$	75%	2.04 $\times$	83.6%	-0.6%
	HASS + TriSpec	89%	<b>3.27</b> $\times$	87%	<b>2.47</b> $\times$	77%	<b>2.74</b> $\times$	87%	<b>2.12</b> $\times$	73%	<b>2.18</b> $\times$	82.6%	-1.6%
	EAGLE3	92%	3.14 $\times$	85%	2.40 $\times$	77%	2.53 $\times$	89%	2.23 $\times$	76%	2.29 $\times$	83.8%	-0.4%
	EAGLE3 + TriSpec	88%	<b>3.40</b> $\times$	87%	<b>2.79</b> $\times$	79%	<b>2.92</b> $\times$	88%	<b>2.36</b> $\times$	72%	<b>2.42</b> $\times$	82.8%	-1.4%
EAGLE3	Single Model (Target,70B)	87%	1.00 $\times$	88%	1.00 $\times$	75%	1.00 $\times$	87%	1.00 $\times$	80%	1.00 $\times$	83.4%	1.00 $\times$
	Single Model (Proxy,8B)	72%	3.80 $\times$	81%	3.92 $\times$	70%	3.95 $\times$	79%	3.93 $\times$	60%	3.96 $\times$	72.4%	-11.0%
	EAGLE3 + TriSpec	86%	<b>3.93</b> $\times$	89%	<b>2.74</b> $\times$	78%	<b>3.06</b> $\times$	89%	<b>2.32</b> $\times$	78%	<b>2.39</b> $\times$	84.0%	+0.6%
													<b>2.89</b> $\times$

## 4. Experiments

### 4.1. Setup

**Models and baselines.** We evaluate TriSpec across three model families: Qwen3, DeepSeek-R1-Distill-Qwen (DSQ), and DeepSeek-R1-Distill-LLaMA (DSL). We pair target models (Qwen3-32B, DSQ-32B, DSL-70B) with their same-family smaller versions as proxies (1.7B, 1.5B, 8B), using corresponding HASS/EAGLE3 weights for drafting. Baselines include standard speculative decoding and SpecCascade (Narasimhan et al., 2024) variants. All drafters are retrained on unified data for fair comparison. Following EAGLE-2 configuration, we set the draft tree depth 6, the expansion top-k 10, and the total draft budget tokens 60. For TriSpec, we employ the margin threshold  $\lambda = 0.5$ . Further details are provided in Appendix B.1 and B.2.

**Benchmarks.** We primarily evaluate our method on five reasoning benchmarks: three mathematical reasoning datasets (GSM8K (Cobbe et al., 2021), MATH500 (Lightman et al., 2023), Gaokao-2023-EN) and two code-generation datasets (HumanEval (Chen et al., 2021), MBPP (Austin et al., 2021)). To further assess performance across diverse domains and more challenging settings, we also include SpecBench (Xia et al., 2024), HotpotQA (Yang et al., 2018), Polymath (Wang et al., 2025b), AIME24&25 (Zhang & Math-AI, 2024), and GPQA-Diamond (Rein et al., 2024). To prevent excessive GPU memory usage, we set the maximum generation length to 8192 tokens. Consistent with prior work (Cai et al., 2024; Li et al., 2025) on speculative decoding, we fix the batch size to 1. Detailed benchmark settings and analysis can be found in Appendix B.3.

**Metrics.** We report pass@1 accuracy for reasoning and LLM-judge scores for SpecBench. Efficiency is measured by throughput (tokens/s, TPS) and speedup relative to target-only decoding. Additionally, we define the target-invocation ratio ( $r_t$ ) as the percentage of target model calls per generated token to quantify verification overhead.

### 4.2. Effectiveness of TriSpec

Table 1 reports the performance and efficiency of TriSpec at a sampling temperature of 0. On all benchmark, TriSpec preserves predictive accuracy with an average degradation within 1%. Concurrently, proxy-side verification delivers significantly higher throughput than standard SD. Specifically, for Qwen3, TriSpec enhances the speedup of HASS from 2.30 $\times$  to 3.26 $\times$  and EAGLE3 from 2.77 $\times$  to 3.55 $\times$ , i.e., roughly a 30% relative improvement. Similar improvements (15%-35%) are observed across the DSQ and DSL families. In contrast, while alternative lossy baselines like SpecCascade offer tunable trade-offs, they generally yield a less optimal balance between accuracy and speedup compared to TriSpec.

Results at temperature 1.0 (Table 2) confirm that TriSpec remains robust under non-deterministic decoding. It consistently provides 10%-35% speedup improvements across all model families while maintaining competitive accuracy, with an average drop of less than 2%. This demonstrates that the confidence-based routing strategy generalizes effectively even to stochastic sampling settings.

Table 3 provides a detailed breakdown of verification efficiency on MATH500 and HumanEval. Compared to standard SD, TriSpec consistently reduces the target-invocation

Table 3. Comparison of per-sample averages across all methods on MATH500 and HumanEval: Target-invocation ratio ( $r_t$ ), average per-round verification time ( $t_v$ ), average acceptance length ( $\tau$ ), Latency( $L$ ), and Speed.

Model	Method	MATH500					HumanEval				
		$r_t$	$t_v$ (s)	$\tau$	$L$ (s)	Speed(Tok/s)	$r_t$	$t_v$ (s)	$\tau$	$L$ (s)	Speed(Tok/s)
Qwen3	Single Model (Target,32B)	100.00%	/	/	258.76	14.24	100.00%	/	/	234.27	14.65
	HASS	25.01%	0.094	4.21	115.04	32.45	27.14%	0.103	3.93	119.32	29.80
	HASS + TriSpec	<b>10.24%</b>	<b>0.070</b>	<b>4.39</b>	<b>83.03</b>	<b>45.26</b>	<b>11.61%</b>	<b>0.077</b>	<b>4.41</b>	<b>78.74</b>	<b>43.38</b>
	EAGLE3	21.38%	0.094	<b>4.72</b>	97.52	38.96	22.05%	0.103	4.60	86.62	39.76
DSQ	EAGLE3 + TriSpec	<b>9.95%</b>	<b>0.071</b>	4.59	<b>74.73</b>	<b>49.74</b>	<b>11.15%</b>	<b>0.080</b>	<b>4.76</b>	<b>71.83</b>	<b>48.00</b>
	Single Model (Target,32B)	100.00%	/	/	156.82	16.82	100.00%	/	/	163.68	17.35
	HASS	22.59%	0.068	<b>4.50</b>	47.92	50.29	23.55%	0.072	<b>4.16</b>	56.75	48.40
	HASS + TriSpec	<b>11.10%</b>	<b>0.054</b>	4.31	<b>43.25</b>	<b>57.30</b>	<b>14.20%</b>	<b>0.061</b>	4.05	<b>52.90</b>	<b>51.15</b>
DSL	EAGLE3	20.67%	0.068	<b>4.79</b>	46.13	53.77	21.45%	0.072	<b>4.54</b>	51.80	53.66
	EAGLE3 + TriSpec	<b>10.63%</b>	<b>0.055</b>	4.78	<b>42.06</b>	<b>60.03</b>	<b>13.25%</b>	<b>0.064</b>	<b>4.54</b>	<b>48.92</b>	<b>57.02</b>
	Single Model (Target,70B)	100.00%	/	/	256.79	8.22	100.00%	/	/	254.18	8.37
	EAGLE3	28.70%	0.144	3.48	108.89	19.33	26.88%	0.147	<b>3.66</b>	107.92	20.84
	EAGLE3 + TriSpec	<b>11.60%</b>	<b>0.093</b>	<b>3.64</b>	<b>78.32</b>	<b>27.54</b>	<b>15.18%</b>	<b>0.114</b>	<b>3.59</b>	<b>87.51</b>	<b>25.70</b>

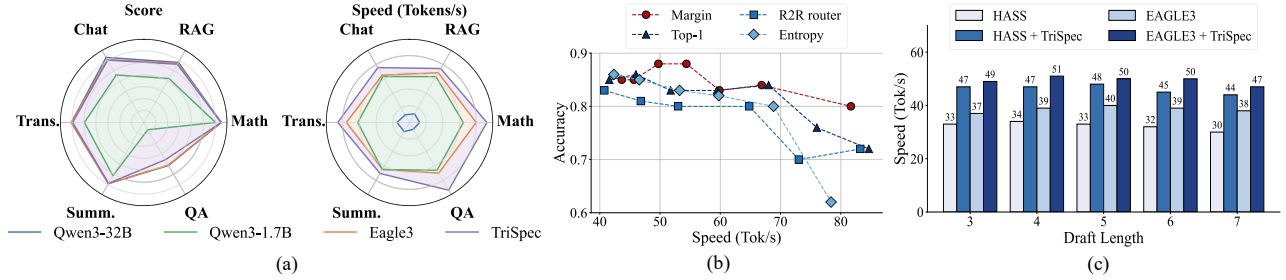


Figure 5. (a) Radar chart illustrating score and speed across all SpecBench subtasks. All experiments are conducted using models from the Qwen3 family. (b) Accuracy–speed trade-offs of different routing strategies. (c) Decoding speed under varying draft lengths for standard speculative decoding and TriSpec. All experiments conducted on the MATH500 dataset using Qwen3-32B as the target.

ratio ( $r_t$ ), per-round verification time ( $t_v$ ), and end-to-end latency ( $L$ ). For instance, on the Qwen3 family, TriSpec nearly halves  $r_t$  while decreasing  $t_v$  from 0.094s to 0.070s, resulting in significantly lower latency. These consistent improvements across all model families demonstrate TriSpec’s effectiveness in shifting the verification workload away from the expensive target model.

Beyond standard reasoning tasks, TriSpec generalizes well to diverse domains and extremely challenging scenarios (Table 4). On SpecBench, TriSpec both robust performance and significant speedup across all sub-tasks as illustrated in Figure 5(a). It similarly sustains gains on difficult benchmarks like AIME and GPQA, demonstrating strong generalization to complex instruction-following and advanced reasoning. Further details are provided in Appendix B.4.

### 4.3. Routing Criteria

We examine both rule-based and training-based routing approaches. To avoid semantic bias from limited-capacity draft models, all routing designs rely exclusively on fea-

tures from the proxy verifier rather than the draft model. Specifically, we evaluate top-1 probability, a composite entropy criterion (Wang et al., 2025a), and the probability margin between the top-two candidates. For training-based routing, we follow the R2R (Fu et al., 2025) to train a lightweight router for cross-model coordination. As shown in Figure 5(b), while all methods can preserve accuracy under calibrated thresholds, margin-based routing offers the most favorable accuracy–speedup trade-off and is thus adopted as the default for TriSpec.

### 4.4. Ablation Studies

**Draft Training Strategies.** TriSpec supports two training paradigms for EAGLE-family draft models to balance draft quality and computational overhead. Joint from-scratch training of the backbone and adapter captures the full synergy between target and proxy features for optimal performance, while adapter-only finetuning provides a cost-effective alternative when pre-trained weights are available. As shown in Table 5 left, while joint training offers slightly

Table 4. Accuracy and speed in general-domain and extremely difficult scenarios.

Method	SpecBench		HotpotQA		Polymath		AIME24		AIME25		GPQA-Diamond	
	Score	Speedup	Acc.	Speedup	Acc.	Speedup	Acc.	Speedup	Acc.	Speedup	Acc.	Speedup
Qwen3	Single Model (Target, 32B)	8.82	1.00×	93.0%	1.00×	27.8%	1.00×	24/30	1.00×	22/30	1.00×	67.2%
	Single Model (Proxy, 1.7B)	7.33	2.72×	84.2%	2.96×	9.4%	3.35×	16/30	3.60×	12/30	3.54×	44.9%
EAGLE3		8.77	2.80×	92.8%	2.77×	27.2%	2.34×	22/30	2.52×	21/30	2.31×	68.2%
EAGLE3+TriSpec		8.62	3.17×	92.8%	3.58×	26.1%	3.11×	23/30	3.37×	21/30	3.30×	66.2%
												4.39×

Table 5. Performance under different draft model training strategies on the Qwen3 family. TP denotes Training Parameters in billions.

Training Strategy	TP	MATH500			HumanEval			Verification strategy	five datasets (avg)		
		$\tau$	$r_t$	Speedup	$\tau$	$r_t$	Speedup		$\tau$	Acc.	Speedup
joint from scratch	1.77	4.59	9.95%	3.49×	4.76	11.1%	3.27×		4.71	84.2%	3.55×
adapter finetuning	0.42	4.52	9.99%	3.44×	4.65	11.4%	3.21×		4.58	84.2%	3.46×

longer acceptance lengths, both strategies consistently deliver end-to-end speeds that substantially exceed standard speculative decoding.

**Token pruning strategies.** Under TriSpec’s Case II, the target model is involved in the verification process. Leveraging the parallelized nature of verification, the target can either validate the entire draft or trust the proxy’s partial verification and only process the remaining tokens, a technique we refer to as token pruning. As demonstrated in Table 5 right, the token pruning strategy enhances the average acceptance length without compromising predictive accuracy. This further underscores the reliability of proxy-side assessments when the proxy exhibits high confidence, allowing the target model to safely bypass redundant computations.

**Draft length.** The draft length per round influences the verification path and attainable speedup. Due to proxy-target behavioral mismatches and the token pruning mechanism, TriSpec’s optimal draft length can differ from standard SD. Figure 5(c) compares throughput for both methods across various draft lengths. For Qwen3 on MATH500, TriSpec is faster at all lengths, and its optimal setting shifts modestly relative to standard SD: from 4 to 5 for HASS-trained drafters and 5 to 4 for EAGLE3.

## 5. Related Work

Beyond the approaches discussed earlier, several lines of work accelerate SD in specific settings. On the drafting side, retrieval-based methods such as REST (He et al., 2023) and LLMA (Yang et al., 2023) identify suitable draft tokens by matching relevant segments from the input context. Cache-reuse approaches, including GLIDE (Du et al., 2024), and MoA (Zimmer et al., 2024), leverage the target model’s KV cache for fast drafting. Techniques like layer-skipping (El-houshi et al., 2024; Zhang et al., 2023) construct simplified draft models by partially reusing the parameters of the target model. Within the single-layer drafter designs, AdaEAGLE (Zhang et al., 2024b) and SpecDec++ (Huang et al.,

2024) dynamically control the draft length to avoid unnecessary computation. On the verification side, Judge Decoding (Bachmann et al., 2025) trains a small judgment model to identify and accept correct but misaligned drafts. Traversal Verify adopts a leaf-to-root procedure for sequence-level verification (Weng et al., 2025). And TriForce (Sun et al., 2024) introduces a hierarchical framework that combines retrieval-based drafting with hierarchical speculation to alleviate KV-cache bottlenecks in long-context settings. Despite these advances, most methods primarily pursue higher acceptance or cheaper drafting; the per-round verification time remains largely unaddressed.

Collaboration between a small language model (SLM) and a large language model (LLM) has been explored for acceleration. R2R (Fu et al., 2025) earns a router to switch between the SLM and LLM. SpecCascade (Narasimhan et al., 2024) combines cascaded inference with speculative decoding to enable cooperative generation. In contrast, we combine the SLM and LLM with an efficient single-layer drafter in a ternary framework, exploiting their alignment to achieve tighter coupling and more effective cooperation.

## 6. Conclusion

In this work, we introduced a new perspective for accelerating speculative decoding by reducing verification time and proposed TriSpec, a ternary framework that combines a lightweight proxy verifier with the drafter and target model. By leveraging same-family smaller models as proxies, TriSpec exploits their strong alignment and reliable outputs to offload a substantial fraction of verification from the target, while a margin-based routing mechanism ensures accuracy is preserved through selective escalation. Extensive experiments show that TriSpec achieves up to 30% additional speedup over standard speculative decoding and sustains accuracy with minimal loss. These results highlight the potential of proxy verification as a new and effective direction for speculative decoding.

## Impact Statement

This work proposes inference acceleration methods for LLMs to improve computational efficiency and scalability, enabling broader deployment by reducing latency and resource consumption. We acknowledge that improved efficiency may also lower the cost of large-scale deployment and could amplify both beneficial and potentially harmful uses; however, these risks are not unique to our methods, and we emphasize the importance of responsible use and adherence to existing safety and governance frameworks. This study follows standard ethical research practices and considers issues related to bias, fairness, privacy, security, and legal compliance. The proposed methods are purely technical and do not introduce new data sources or modify training data, and the authors declare no conflicts of interest.

## References

Austin, J., Odena, A., Nye, M., Bosma, M., Michalewski, H., Dohan, D., Jiang, E., Cai, C., Terry, M., Le, Q., et al. Program synthesis with large language models. *arXiv preprint arXiv:2108.07732*, 2021.

Bachmann, G., Anagnostidis, S., Pumarola, A., Georgopoulos, M., Sanakoyeu, A., Du, Y., Schönfeld, E., Thabet, A., and Kohler, J. Judge decoding: Faster speculative sampling requires going beyond model alignment. *arXiv preprint arXiv:2501.19309*, 2025.

Cai, T., Li, Y., Geng, Z., Peng, H., Lee, J. D., Chen, D., and Dao, T. Medusa: Simple llm inference acceleration framework with multiple decoding heads. *arXiv preprint arXiv:2401.10774*, 2024.

Chen, C., Borgeaud, S., Irving, G., Lespiau, J.-B., Sifre, L., and Jumper, J. Accelerating large language model decoding with speculative sampling. *arXiv preprint arXiv:2302.01318*, 2023.

Chen, M., Tworek, J., Jun, H., Yuan, Q., Pinto, H. P. D. O., Kaplan, J., Edwards, H., Burda, Y., Joseph, N., Brockman, G., et al. Evaluating large language models trained on code. *arXiv preprint arXiv:2107.03374*, 2021.

Cobbe, K., Kosaraju, V., Bavarian, M., Chen, M., Jun, H., Kaiser, L., Plappert, M., Tworek, J., Hilton, J., Nakano, R., et al. Training verifiers to solve math word problems. *arXiv preprint arXiv:2110.14168*, 2021.

Ding, N., Chen, Y., Xu, B., Qin, Y., Zheng, Z., Hu, S., Liu, Z., Sun, M., and Zhou, B. Enhancing chat language models by scaling high-quality instructional conversations. *arXiv preprint arXiv:2305.14233*, 2023.

Du, C., Jiang, J., Yuanchen, X., Wu, J., Yu, S., Li, Y., Li, S., Xu, K., Nie, L., Tu, Z., et al. Glide with a cape: A low-hassle method to accelerate speculative decoding. *arXiv preprint arXiv:2402.02082*, 2024.

Elhoushi, M., Shrivastava, A., Liskovich, D., Hosmer, B., Wasti, B., Lai, L., Mahmoud, A., Acun, B., Agarwal, S., Roman, A., et al. Layerskip: Enabling early exit inference and self-speculative decoding. *arXiv preprint arXiv:2404.16710*, 2024.

Fu, T., Ge, Y., You, Y., Liu, E., Yuan, Z., Dai, G., Yan, S., Yang, H., and Wang, Y. R2r: Efficiently navigating divergent reasoning paths with small-large model token routing. *arXiv preprint arXiv:2505.21600*, 2025.

Grattafiori, A., Dubey, A., Jauhri, A., Pandey, A., Kadian, A., Al-Dahle, A., Letman, A., Mathur, A., Schelten, A., Vaughan, A., et al. The llama 3 herd of models. *arXiv preprint arXiv:2407.21783*, 2024.

He, Z., Zhong, Z., Cai, T., Lee, J. D., and He, D. Rest: Retrieval-based speculative decoding. *arXiv preprint arXiv:2311.08252*, 2023.

Huang, K., Guo, X., and Wang, M. Specdec++: Boosting speculative decoding via adaptive candidate lengths. *arXiv preprint arXiv:2405.19715*, 2024.

Leviathan, Y., Kalman, M., and Matias, Y. Fast inference from transformers via speculative decoding. In *International Conference on Machine Learning*, pp. 19274–19286. PMLR, 2023.

Li, Y., Wei, F., Zhang, C., and Zhang, H. Eagle: Speculative sampling requires rethinking feature uncertainty. *arXiv preprint arXiv:2401.15077*, 2024a.

Li, Y., Wei, F., Zhang, C., and Zhang, H. Eagle-2: Faster inference of language models with dynamic draft trees. *arXiv preprint arXiv:2406.16858*, 2024b.

Li, Y., Wei, F., Zhang, C., and Zhang, H. Eagle-3: Scaling up inference acceleration of large language models via training-time test. *arXiv preprint arXiv:2503.01840*, 2025.

Lightman, H., Kosaraju, V., Burda, Y., Edwards, H., Baker, B., Lee, T., Leike, J., Schulman, J., Sutskever, I., and Cobbe, K. Let's verify step by step. In *The Twelfth International Conference on Learning Representations*, 2023.

Liu, A., Feng, B., Xue, B., Wang, B., Wu, B., Lu, C., Zhao, C., Deng, C., Zhang, C., Ruan, C., et al. Deepseek-v3 technical report. *arXiv preprint arXiv:2412.19437*, 2024.

Narasimhan, H., Jitkrittum, W., Rawat, A. S., Kim, S., Gupta, N., Menon, A. K., and Kumar, S. Faster cascades via speculative decoding. *arXiv preprint arXiv:2405.19261*, 2024.

Rein, D., Hou, B. L., Stickland, A. C., Petty, J., Pang, R. Y., Dirani, J., Michael, J., and Bowman, S. R. Gpqa: A graduate-level google-proof q&a benchmark. In *First Conference on Language Modeling*, 2024.

Sun, H., Chen, Z., Yang, X., Tian, Y., and Chen, B. Tri-force: Lossless acceleration of long sequence generation with hierarchical speculative decoding. *arXiv preprint arXiv:2404.11912*, 2024.

Wang, J., Tian, Z., Li, J., Xia, Q., Duan, X., Wang, Z., Huai, B., and Zhang, M. Alignment-augmented speculative decoding with alignment sampling and conditional verification. *arXiv preprint arXiv:2505.13204*, 2025a.

Wang, Y., Zhang, P., Tang, J., Wei, H., Yang, B., Wang, R., Sun, C., Sun, F., Zhang, J., Wu, J., et al. Polymath: Evaluating mathematical reasoning in multilingual contexts. *arXiv preprint arXiv:2504.18428*, 2025b.

Weng, Y., Hu, Q., Chen, X., Liu, L., Mei, D., Qiu, H., Tian, J., and Shi, Z. Traversal verification for speculative tree decoding. *arXiv preprint arXiv:2505.12398*, 2025.

Xia, H., Yang, Z., Dong, Q., Wang, P., Li, Y., Ge, T., Liu, T., Li, W., and Sui, Z. Unlocking efficiency in large language model inference: A comprehensive survey of speculative decoding. *arXiv preprint arXiv:2401.07851*, 2024.

Yang, A., Li, A., Yang, B., Zhang, B., Hui, B., Zheng, B., Yu, B., Gao, C., Huang, C., Lv, C., et al. Qwen3 technical report. *arXiv preprint arXiv:2505.09388*, 2025.

Yang, N., Ge, T., Wang, L., Jiao, B., Jiang, D., Yang, L., Majumder, R., and Wei, F. Inference with reference: Lossless acceleration of large language models. *arXiv preprint arXiv:2304.04487*, 2023.

Yang, Z., Qi, P., Zhang, S., Bengio, Y., Cohen, W., Salakhutdinov, R., and Manning, C. D. Hotpotqa: A dataset for diverse, explainable multi-hop question answering. In *Proceedings of the 2018 conference on empirical methods in natural language processing*, pp. 2369–2380, 2018.

Zhang, J., Wang, J., Li, H., Shou, L., Chen, K., Chen, G., and Mehrotra, S. Draft & verify: Lossless large language model acceleration via self-speculative decoding. *arXiv preprint arXiv:2309.08168*, 2023.

Zhang, L., Wang, X., Huang, Y., and Xu, R. Learning harmonized representations for speculative sampling. *arXiv preprint arXiv:2408.15766*, 2024a.

Zhang, S., Wang, H., Ma, D., Zhu, Z., Chen, L., Lan, K., and Yu, K. Adaeagle: Optimizing speculative decoding via explicit modeling of adaptive draft structures. *arXiv preprint arXiv:2412.18910*, 2024b.

Zhang, Y. and Math-AI, T. American invitational mathematics examination (aime) 2024, 2024.

Zheng, L., Chiang, W.-L., Sheng, Y., Zhuang, S., Wu, Z., Zhuang, Y., Lin, Z., Li, Z., Li, D., Xing, E., et al. Judging llm-as-a-judge with mt-bench and chatbot arena. *Advances in neural information processing systems*, 36: 46595–46623, 2023.

Zimmer, M., Gritta, M., Lampouras, G., Ammar, H. B., and Wang, J. Mixture of attentions for speculative decoding. *arXiv preprint arXiv:2410.03804*, 2024.

## A. Algorithm

Algorithm 1 provides the formal pseudo-code for a single generation round of TriSpec. It specifies the autoregressive drafting process, proxy-based pre-verification, and margin-based routing logic for conditional target escalation.

---

### Algorithm 1 TriSpec in a single round

---

```

1: Inputs: Draft model  $\mathcal{M}_d$ , Proxy verifier  $\mathcal{M}_p$ , Target model  $\mathcal{M}_t$ , input prefix  $X$ , margin-based threshold  $\lambda$ 
   # Sample  $k$  draft tokens from  $\mathcal{M}_d$  autoregressively
2: for  $i = 1$  to  $k$  do
3:    $\mathbf{p}_i^{(d)} \leftarrow \mathcal{M}_d(X + [x_1, \dots, x_{i-1}])$ 
4:    $x_i \sim \mathbf{p}_i^{(d)}$ 
5: end for

   # Pre-verification by  $\mathcal{M}_p$ 
6:  $\tau_a, [\mathbf{p}_1^{(p)}, \dots, \mathbf{p}_{k+1}^{(p)}] \leftarrow \text{Verify}(\mathcal{M}_p, X + [x_1, \dots, x_k])$ 
   # Determine proxy-trusted length via margin-based rule
7:  $g(\mathbf{p}_i^{(p)}) \leftarrow \mathbf{1}\left\{\text{top}_1(\mathbf{p}_i^{(p)}) - \text{top}_2(\mathbf{p}_i^{(p)}) \geq \lambda\right\}, i = 1, \dots, k+1$ 
8:  $\tau_m \leftarrow \min(\{i \mid 0 \leq i \leq k, g(\mathbf{p}_{i+1}^{(p)}) = 0\} \cup \{k+1\})$ 
   # Conditional routing to target based on proxy reliability
9: if  $\tau_a < \tau_m$  then
10:   $x_{\text{bonus}} \sim \mathbf{p}_{\tau_a+1}^{(p)}$ 
11:  return  $X + [x_1, \dots, x_{\tau_a}, x_{\text{bonus}}]$ 
12: else
13:   $\tau_t, [\mathbf{p}_{\tau_m+1}^{(t)}, \dots, \mathbf{p}_{k+1}^{(t)}] \leftarrow \text{Verify}(\mathcal{M}_t, X + [x_1, \dots, x_k])$ 
14:   $x_{\text{bonus}} \sim \mathbf{p}_{\tau_m+\tau_t+1}^{(t)}$ 
15:  return  $X + [x_1, \dots, x_{\tau_m+\tau_t}, x_{\text{bonus}}]$ 
16: end if

```

---

## B. Experimental Details and Additional Experimental Results

### B.1. Draft training details

We follow the HASS/EAGLE-3 official codebases and guidelines from the respective papers to train the draft models. In TriSpec, the drafter’s backbone and adapter are jointly trained from scratch. Specifically, HASS is trained on 68K ShareGPT examples, and EAGLE3 additionally incorporates UltraChat-200K (Ding et al., 2023). Concretely, we first generate responses autoregressively with the target model and then compute token-level hidden features offline with both the proxy and the target to supervise baseline training and our adapter. Training is performed on  $8 \times$  NVIDIA A100 80GB GPUs, with hyperparameters set according to the official default settings unless otherwise noted. Notably, during the EAGLE3 training process, we maintain a full vocabulary for training and set the batch size to 1 to avoid out-of-memory errors. In terms of training time, for the 32B target model, HASS/EAGLE3 typically requires 3-4 days, while TriSpec takes approximately 4-5 days due to the additional requirement of training the proxy’s features. The details of the training cost are shown in Table 6.

During inference, we follow the scripts provided by the official EAGLE implementation. All benchmark inference experiments are conducted on a single NVIDIA A100 80GB GPU.

Table 6. Training cost of EAGLE3 and TriSpec on Qwen3 family

Method	Training Strategy	Data Size	Seq Len	TP(B)	Epochs	Training Time(h)
EAGLE3	/	518K	2048	1.35	6	78
EAGLE3 + TriSpec	joint-training from scratch	518K	2048	1.77	6	115
EAGLE3 + TriSpec	adapter-only finetune	518K	2048	0.42	3	44

## B.2. Baseline Implementation Details: SpecCascade

We adopt SPECCASCADE as one of our main baselines. SPECCASCADE encompasses various rule-based strategies for relaxed verification within speculative decoding. In our experiments, we implement three representative *deferral rules*:

- **Chow rule:** This method compares the probability assigned by the draft model to a candidate token against a fixed threshold, accepting the token if it exceeds this threshold (see Table 1 in the original SpecCascade paper). Notably, our *confidence-filter* method described in Appendix C.2 is equivalent to the Chow rule.
- **Optimal deferral rule:** This method compares the probability assigned by the draft model to the maximum probability from the target model’s distribution. The rejection threshold in this method is determined as a function of the distance between the two distributions (see Eq. (10) in the original paper).
- **Token-specific deferral rule:** This method decides acceptance by comparing the probability of the candidate token in the target model’s distribution against the target’s maximum probability. It does not use the draft model’s output distribution at all (see Eq. (14) in the original paper).

In our implementation, we set a small  $\alpha = 0.05$  for rules relying on the draft model’s output distribution (Chow and Optimal deferral), and a relatively larger  $\alpha = 0.2$  for the token-specific deferral rule.

As shown in Table 1, when the draft model is a *small single-layer* architecture, deferral rules that rely on the draft model’s probability severely harm accuracy: even with very small  $\alpha$ , Chow and Optimal deferral rules still incur substantial degradation, consistent with our findings in Appendix C.2. In contrast, the token-specific deferral rule maintains accuracy by relying solely on the target model’s distribution. However, because the small drafter can only produce a limited number of high-quality tokens, the resulting speedup gains from this rule are modest.

## B.3. Standard Reasoning Benchmark Details and Statistical Robustness Analysis

To manage the substantial inference costs associated with large-scale reasoning models, we primarily conduct our evaluations on randomly sampled subsets of 100 examples from each reasoning benchmark. These subsets serve as the basis for all experimental results reported in the main text. This strategy allows for a broad and computationally feasible comparison across multiple model families and diverse tasks. For the Qwen3 model family, however, we additionally extend the evaluation to the full set of benchmarks to provide a more comprehensive performance profile. The results on these complete test sets are reported in Table 7, which demonstrate that the performance and efficiency gains observed in our 100-sample subsets remain consistent across the full datasets.

To further ensure the stability and reliability of our findings, we perform repeated evaluations on the GSM8K benchmark by drawing eight distinct random subsets of 100 samples each. As shown in Figure 6, we compute the mean results and include error bars denoting one standard deviation across these independent runs. Both the full-benchmark evaluations and the repeated-subset experiments consistently show that TriSpec achieves substantially higher generation speeds than standard speculative decoding, with only minor accuracy degradation. The narrow error bars further indicate that performance variations introduced by random sampling are negligible, confirming that our main conclusions are robust and not an artifact of subset selection.

Table 7. Accuracy and speedup results on the full benchmark suite for Qwen3 family

Method	GSM8K		MATH500		Gaokao2023en		HumanEval		MBPP	
	Acc.	Speedup	Acc.	Speedup	Acc.	Speedup	Acc.	Speedup	Acc.	Speedup
Single Model (Target, 32B)	94.9%	1.00 $\times$	86.8%	1.00 $\times$	78.2%	1.00 $\times$	86.6%	1.00 $\times$	74.8%	1.00 $\times$
Single Model (Proxy, 1.7B)	86.0%	2.52 $\times$	78.2%	2.87 $\times$	69.9%	2.76 $\times$	77.4%	2.87 $\times$	52.8%	2.93 $\times$
EAGLE3	94.3%	3.29 $\times$	88.0%	2.77 $\times$	77.1%	2.77 $\times$	87.2%	2.72 $\times$	74.2%	2.71 $\times$
EAGLE3 + TriSpec	92.9%	<b>4.08</b> $\times$	87.4%	<b>3.48</b> $\times$	77.4%	<b>3.39</b> $\times$	86.0%	<b>3.23</b> $\times$	71.4%	<b>3.33</b> $\times$

## B.4. Implementation Details of General and Extremely Difficult Benchmarks

This section provides comprehensive descriptions and implementation protocols for the benchmarks used to assess TriSpec’s performance across general domains and frontier-level reasoning challenges. These datasets include SpecBench, HotpotQA,

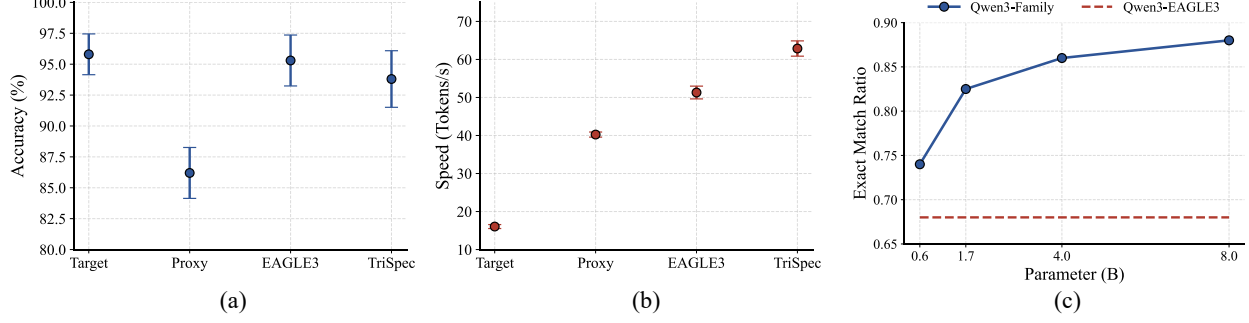


Figure 6. (a-b) Error bars (one standard deviation) of accuracy and speed for four generation methods across repeated random subset sampling. (c) Token-level exact match ratios of models with varying parameter scales and the EAGLE3 drafter, computed using Qwen3-32B predictions as reference.

Polymath, AIME 2024, AIME 2025, and GPQA-Diamond.

SpecBench comprises 480 samples spanning six categories: multi-turn conversation, translation, summarization, question answering (QA), mathematical reasoning, and retrieval-augmented generation (RAG). Within the multi-turn conversation category, the benchmark includes diverse open-ended tasks such as writing, roleplay, extraction, and humanities. This benchmark offers a comprehensive evaluation of model performance across a wide range of domains. HotpotQA is a natural-language, multi-hop question answering benchmark with explicit supporting-fact supervision, offering a distinct QA format compared to SpecBench, for which we evaluate on a subset of 500 randomly selected samples. Polymath is a multilingual mathematical reasoning benchmark covering 18 languages and four difficulty levels. To assess performance in multilingual and extremely challenging scenarios, we sample 20 high-difficulty instances from each language, yielding 360 test samples in total. AIME-24 and AIME-25 are widely recognized as highly challenging mathematical reasoning benchmarks, with problems drawn from the American Invitational Mathematics Examination. Each dataset consists of 30 competition-level problems. GPQA-Diamond is the high-quality subset of the GPQA benchmark, comprising 198 expert-written multiple-choice questions spanning biology, physics, and chemistry. For these datasets, we evaluate on the full test sets to further assess the robustness of our method under extremely challenging problem settings.

For SpecBench, given that most tasks are open-ended, we adopt the LLM-judge protocol from FastChat (Zheng et al., 2023), using GPT-4.1 as the judgment model to score responses from 0 to 10 on a per-turn basis. For others, we use accuracy as the evaluation metric.

## B.5. Experiments on Non-Reasoning Models

We further evaluate TriSpec on non-reasoning models by using LLaMA-3.1-8B and LLaMA-3.2-1B as the target model and the proxy verifier, respectively. The results in Table 8 show that TriSpec remains effective on these non-reasoning model families, maintaining accuracy close to that of the target while providing faster verification compared to standard SD.

Table 8. Accuracy and speedup results for original LLaMA3 family

Method	GSM8K		MATH500		Gaokao2023en		HumanEval		MBPP	
	Acc.	Speedup	Acc.	Speedup	Acc.	Speedup	Acc.	Speedup	Acc.	Speedup
Single Model (Target, 8B)	64%	1.00 $\times$	34%	1.00 $\times$	18%	1.00 $\times$	66%	1.00 $\times$	57%	1.00 $\times$
Single Model (Proxy, 1B)	34%	2.54 $\times$	26%	2.53 $\times$	10%	2.50 $\times$	46%	2.58 $\times$	29%	2.53 $\times$
HASS	64%	2.93 $\times$	34%	3.27 $\times$	18%	3.23 $\times$	66%	3.52 $\times$	57%	3.46 $\times$
HASS + TriSpec	62%	<b>3.17<math>\times</math></b>	34%	<b>3.73<math>\times</math></b>	17%	<b>3.66<math>\times</math></b>	66%	<b>3.81<math>\times</math></b>	54%	<b>3.76<math>\times</math></b>

## B.6. Proxy selection in TriSpec

Figure 6(c) compares the token-level exact match ratio between Qwen3 models of varying parameter counts and the Qwen3-32B target model. Match ratios increase with model size, but the marginal gains diminish beyond the 1.7B scale. Since token-level alignment directly impacts a proxy’s ability to assist the target in verification, this trend is a key factor

in proxy selection. In particular, the 0.6B model surpasses the single-layer EAGLE3 drafter by only about 6%, yielding relatively few local corrections. Conversely, the 4B model offers merely a 2.5% increase over the 1.7B model, yet incurs substantially higher inference overhead. Balancing speed and alignment effectiveness, we adopt the 1.7B model as the proxy in our main experiments.

## C. Further Analysis of the Three Models in TriSpec

### C.1. Standalone examples

Figure 7 shows a case of individual inferences made by the three models used in TriSpec within the Qwen3 family. The smaller model from the same family (Qwen3-1.7B, proxy verifier) are implicitly aligned with the target model (Qwen3-32B), exhibiting notable similarity in response format and language style, reflecting their strong alignment. Additionally, the smaller model demonstrates reasonable inference capabilities. While there are token-level differences compared to the target model, they are still able to produce correct answers, showcasing the reliability of their outputs.

In contrast, the single-layer drafter (EAGLE3), although trained to mimic the target model’s behavior, suffers from weaker contextual understanding due to the significant reduction in attention computations. Without periodic supervision from the target model during generation, the outputs often become illogical.

Query: Calculate  $55^2 - 25^2$

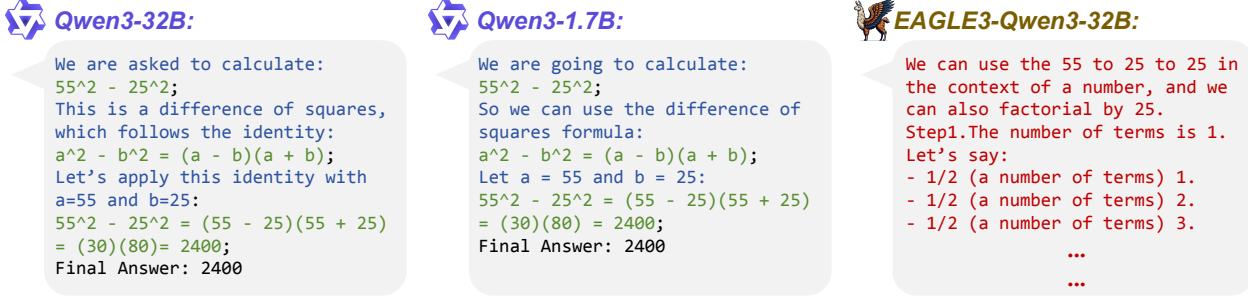


Figure 7. An example of standalone inference for the three models in TriSpec.

### C.2. Token-level alignment experiments

**Experiment details** To compare token-level alignment between the proxy verifier and the target model, we use the ShareGPT dataset as a reference. First, we use Qwen3-32B as the target model to generate autoregressive answers for each prompt. Then, we prefill the target completions using Qwen3-1.7B (the proxy) and record the proxy’s next-token prediction at each position. A token is considered an exact match if the proxy and target predictions coincide. For positions where they differ, we consult a stronger judge (Qwen3-235B) with top-k = 3 and top-p = 0.9 sampling parameters: if the proxy’s token is included in the set of tokens generated under these conditions, we deem it acceptable; otherwise, it is considered unacceptable. For both the proxy and the target model, temperature = 0 is used to ensure deterministic outputs.

**Case Analysis** We also performed token-level alignment comparisons for the single-layer drafter (EAGLE3) and present a case in Figure 8, showcasing the token-level outputs of the three models along with their corresponding confidence scores. The proxy verifier typically shows higher confidence for tokens that are exact matches, and slightly lower confidence for mismatched tokens, demonstrating the reliability of its judgments. Overall, the proxy verifier outperforms the EAGLE3 drafter in alignment (82% vs. 68%). This advantage is particularly evident for decision-critical tokens (e.g., “\*” and “78”), enabling the proxy verifier to locally correct errors made by the single-layer drafter in certain cases. Additionally, due to its limited capacity, the single-layer drafter exhibits overconfidence in certain cases, making its confidence scores unreliable as a basis for determining whether its outputs are acceptable.

Query	Calculate the sum of 1 to 12									
Target model output	... So sum = 1 2 * 1 3 / 2 = 7 8. Let me verify that: 1 + 1 2 = 1 3 ...									
Small model prefill (82% matching ratio)	... So sum = 1 2 * 1 3 / 2 = 7 8. So me verify that: 1 + 1 2 = 1 3 ...									
Confidence	0.76	0.86	0.98		0.92	0.49		0.82	0.85	
Target output	... So sum = 1 2 * 1 3 / 2 = 7 8. Let me verify that: 1 + 1 2 = 1 3 ...									
EAGLE3 prefill (68% matching ratio)	... So that is 1 2 + 1 3 / 2 = 6 8. So me verify that: 1 2 2 2 = 1 3 ...									
Confidence	0.56	0.68	0.89		0.88	0.37		1.00	0.59	

Figure 8. Token-level comparison of three models in TriSpec. Blue highlights mark acceptable mismatch tokens, and red highlights mark unacceptable mismatches. The reported matching ratios are measured on all ShareGPT samples.

### C.3. Attempts at relaxing verification

This work primarily focuses on the verification side, aiming to accelerate SD by relaxing strict verification constraints. In addition to the proxy-based verification used in TriSpec, another natural approach is to relax verification conditions to increase acceptance length, thereby achieving acceleration. We examine two common relaxations in the SD pipeline: (i) confidence filtering, which accepts a drafter token when the drafter’s confidence score ( $\max p_i$ ) exceeds a threshold and skips target verification, and (ii) top- $k$  verification, which accepts the drafter token if it lies within the top- $k$  candidates of the target model. We experiment by separately using single-layer drafters (HASS/EAGLE3 weights) and same-family smaller models as draft models. In these experiments, we use a chain-based draft structure, with the draft length set to 3.

**Single-layer drafter is difficult to relax.** As shown in Figure 9(b), single-layer drafters degrade rapidly under both settings. Confidence filtering admits high-confidence but incorrect drafts because the single-layer drafter is capacity-limited and often overconfident. Top- $k$  verification is brittle, as it can accept incorrect near-optimal tokens, which single-layer drafters frequently emit at decision-critical positions. Consequently, for single-layer drafters, relaxed verification is fragile, and small relaxations already induce noticeable accuracy loss, which limits further acceleration.

In our benchmark evaluation, we comprehensively assess the confidence-filter method across multiple benchmarks, with results reported in Table 1. Despite setting a relatively high threshold of 0.95, the relaxed verification based on the confidence filter still struggles to maintain accuracy. In particular, it frequently induces repeated outputs, which we attribute to the single-layer drafter’s unwarranted overconfidence discussed in Appendix C.2. This is also why we do not rely on feature signals from the draft model when designing the routing strategy.

**High-confidence mismatches in same-family smaller models can be tolerated.** Relaxing verification for smaller models from the same family, when using an appropriate threshold, does not lead to significant accuracy loss. This end-to-end experiment shows that high-confidence mismatches in smaller models can typically be tolerated, further supporting their rationale as proxy verifiers. A similar conclusion is also mentioned in the Judge Decoding (Bachmann et al., 2025).

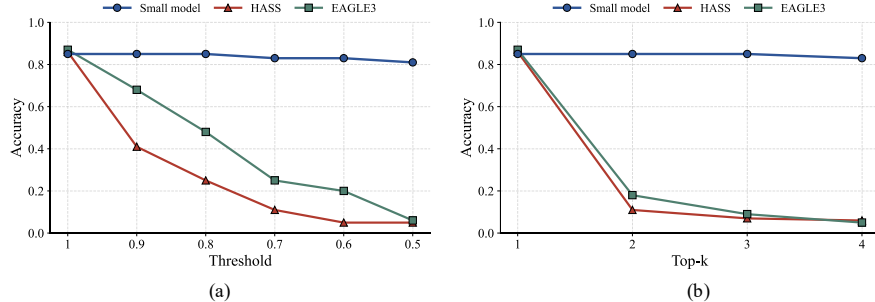


Figure 9. Verification relaxation in the Qwen3 family on the MATH500 dataset. (a) Results with confidence filtering across different confidence thresholds. (b) Results with top- $k$  verification across different  $k$  values.

## D. Case Study of Complete Generation

We present a TriSpec case study of complete generation and compare it with target-only and proxy-only decoding results (Figure 10). Tokens in blue denote outputs verified or generated by the proxy model (DSQ-1.5B), while tokens in black indicate those verified or generated by the target model (DSQ-32B). In this example, over half of the tokens are validated by the proxy model, highlighting TriSpec’s efficiency. When the proxy alone would err, TriSpec attains correctness by involving the target, preserving accuracy.

Specifically, the yellow boxes highlight disagreements between the two models. The proxy incorrectly predicts “He runs 3 sprints each week” instead of the correct “He runs 3 sprints each session.” In TriSpec inference, however, the proxy expresses uncertainty at this point and defers to the target model, thereby avoiding the error and showcasing strong robustness.

**Case: GSM8K**

**Question:** James decides to run 3 sprints 3 times a week. He runs 60 meters each sprint. How many total meters does he run a week?

**GT:** 540

---

**DSQ-32B**

First, I need to determine the total number of sprints James runs each week. He runs 3 sprints each session and does this 3 times a week. So, the total number of sprints is 3 multiplied by 3, which equals 9 sprints.

Next, I need to calculate the total distance James runs. Each sprint is 60 meters, and he completes 9 sprints in total. Therefore, the total distance is 60 meters multiplied by 9, which equals 540 meters.

Finally, the total number of meters James runs each week is 540 meters.

Solution:

To determine the total number of meters James runs in a week, follow these steps:

1. Calculate the total number of sprints per week:  
James runs 3 sprints each session and does this 3 times a week.  
 $Total\ sprints = 3\ sprints/session \times 3\ sessions/week = 9\ sprints/week$
2. Determine the total distance run per week:  
Each sprint is 60 meters. Therefore, the total distance is:  
 $Total\ distance = 9\ sprints \times 60\ meters/sprint = 540\ meters$

Final Answer:  
540

---

**DSQ-1.5B**

I need to determine how many total meters James runs in a week. He runs 3 sprints each week and each sprint is 60 meters long. To find the total distance, I’ll multiply the number of sprints by the distance per sprint.

So, 3 sprints multiplied by 60 meters per sprint equals 180 meters. Therefore, James runs a total of 180 meters each week.

James runs 3 sprints each week, with each sprint being 60 meters long. To find the total distance he runs in a week, multiply the number of sprints by the distance per sprint.

$Total\ meters = Number\ of\ sprints \times Distance\ per\ sprint = 3 \times 60 = 180$

180

---

**TriSpec**

First, I need to determine the total number of sprints James runs in a week. He runs 3 sprints each session and does this 3 times a week. So, the total number of sprints is 3 multiplied by 3, which equals 9 sprints.

Next, each sprint is 60 meters long. To find the total distance James runs in a week, I multiply the number of sprints by the distance of each sprint. That is 9 sprints multiplied by 60 meters per sprint, resulting in 540 meters.

Therefore, James runs a total of 540 meters each week.

Solution:

To determine the total number of meters James runs in a week, follow these steps:

1. Calculate the total number of sprints per week:  
James runs 3 sprints each session and does this 3 times a week.  
 $Total\ sprints\ per\ week = 3\ sprints/session \times 3\ sessions/week = 9\ sprints/week$
2. Determine the total distance run per sprint:  
James runs 60 meters per sprint
3. Calculate the total distance run in a week:  
Multiply the total number of sprints by the distance per sprint.  
 $Total\ distance = 9\ sprints \times 60\ meters/sprint = 540\ meters$

Final Answer:  
540

Figure 10. Case study of TriSpec in GSM8K.